An innovative quad-rotor UAV: design and experiment

Elisa Capello[*], Alessandro Scola[†], Giorgio Guglieri[‡], Fulvia Quagliotti[§]
Politecnico di Torino, Italy

In the last years small and mini UASs have been the subject of several recent research projects, due to their capability to accomplish multi-role missions in very restricted and indoor environments. A new-layout quadrotor mini UAS has been designed at Politecnico di Torino and a suitable flight control system has been developed. The quadrotor dimensions and the structure geometrical properties have been decided in the design process, to withstand the imposed loads. For the prototype, commercial and RC on-board equipments have been selected to simplify the construction and to reduce the overall costs, whereas the controller board has been conceived and customized. The mathematical model, describing the flight dynamics of the mini quadrotor, has been developed. A control strategy with a state feedback controller has been implemented, assigning a robust eigenstructure and the desired dynamic specifications. An adaptive algorithm, which guarantees uniformly bounded response for both the inputs and the outputs, has been presented. A L1 adaptive controller has been studied, including the state predictor, the adaptive and the control laws.

http://www.imavs.org/

Nomenclature

a	=	lift slope	[rad^{-1}]
C	=	reaction torque	[Nm]
CG	=	center of gravity	[-]
C_D	=	blade drag coefficient	[-]
C_L	=	blade lift coefficient	[-]
dD	=	infinitesimal drag	[N]
dL	=	infinitesimal lift	[N]
g	=	acceleration of gravity	[m/s^2]
I_X, I_Y ,I_Z	=	moments of inertia along X, Y, Z axes respectively	[kgm^2]
K_g	=	feedforward pre-filter	[-]
M_w	=	stability static derivative	[-]
MRAC	=	Model Reference Adaptive Control	[-]
p, q and r	=	roll, pitch and yaw angular velocities respectively	[rad/s]
R	=	rotor radius	[m]
R^i_j	=	transformation matrix from i-th frame to j-th frame	[-]
T_i	=	thrust on the i-th propeller	[N]
U_0	=	asymptotic airspeed	[m/s]
w	=	speed along Z axis	[m/s]
β_0	=	reference blade flapping angle	[rad]
λ	=	inflow	[rad/s]
ρ	=	air density	[kg/m^3]
φ, θ and ψ	=	Euler angles	[rad]
ψ	=	azimuth angle	[rad]
Ω	=	propeller angular velocity	[rad/s]

[*] Ph.D Student, Aerospace Engineering Department, Corso Duca degli Abruzzi, 24, 10129 Torino
[†] Graduated Research Assistant, Aerospace Engineering Department, Corso Duca degli Abruzzi, 24, 10129 Torino
[‡] Associate Professor, Aerospace Engineering Department, Corso Duca degli Abruzzi, 24, 10129 Torino
[§] Associate Professor, Aerospace Engineering Department, Corso Duca degli Abruzzi, 24, 10129 Torino

http://www.imavs.org/

I. Introduction

In the last years small Unmanned Aerial Vehicles (UAVs) have been developed for large-scale territorial monitoring. Commercial and civilian sectors refer to small vertical take-off and landing (VTOL) vehicles capable to reduce room take-off and landing, to fly over a target and complete many tasks, without the need for excess manpower or risk of life. For this reason, small rotary wing UAVs have been the subject of several recent research projects. Due to the complexity in control and to the intrinsic instabilities of this type of small size vehicles, multi rotor unmanned vehicles have been developed[1,2,3,4].

Small quadrotors have many exciting potential missions including flight indoors and in urban areas. A quadrotor might achieve stable hovering and precise flight by balancing the forces produced by the four rotors. However the on board software will have to be very compact to fit in the available memory of the small microprocessors, but powerful enough to provide control with sensor data of limited quality.

A quadrotor has four motors located at the front, rear, left, and right ends of a cross frame. The quadrotor is controlled by changing the speed of rotation of each motor. The front and rear rotors rotate in a direction, e.g. counter-clockwise direction, while the left and right rotors rotate in the opposite direction, to balance the torque created by the spinning rotors. The relative speed of the front and rear rotors is varied to control the pitch rate of the UAV. Increasing the speed of the front motor by the same amount that the speed of the rear one is decreased will keep the total thrust provided by the four rotors constant. Furthermore, the total torque created by these two rotors will remain constant. Similarly, the roll rate is controlled by varying the relative speed of the left and right rotors. The yaw rate is controlled by varying the relative speed of the clockwise (right and left) and counter-clockwise (front and rear) rotors. The collective thrust is controlled by varying the speed of all the rotors simultaneously.

The Aerospace Engineering Department (DIASP) of Politecnico di Torino is working on the development of a multi rotor UAV for territorial monitoring and map project for a dead zone[5]. The goals for this platform have to make a system that can be used by a single operator and can stay in a backpack. The research is oriented to analyze the ways to pilot and control this platform. To improve the results a small, robust and highly manoeuvrable UAV is designed and produced, considering the dynamic equations and the performances.

II. The on board controller

The quadrotor flight control has been entrusted to the on board controller.

This controller is needed for two reasons:

- for mixing the command signals received from the on-board receiver. These input signals are sent by a ground operator with a transmitter, moving the stick to perform the requested manouevre,
- for performing the feedback control to assure a stable flight or maintain a desired attitude and position, if these characteristics are implemented.

As a first step, a commercial off the shelf controller board has been searched; due to the inability to customized the control algorithm, implemented on the board, a custom-made controller has been produced. Specifically, the research main topics are the flight testing of 1) different feedback control laws, 2) autonomous flight mode and 3) formation flight.

In Figure 1 is shown the functional scheme of the controller board as scheduled initially. To obtain the desired flight parameters, two sensors are used: three-axes accelerometers and a single-axis gyroscope.

From the accelerometers the pitch and bank angles are derived reversing through the classical equations of dynamics for a rigid body[7,10]. Thus, a single-axis gyroscope is needed to measure the yaw rate so it is possible to compute the yaw Euler angle rate, using the kinematic equation

$$\dot{\Psi} = q \sin\Phi / \cos\Theta + r \cos\Phi / \cos\Theta \tag{1}$$

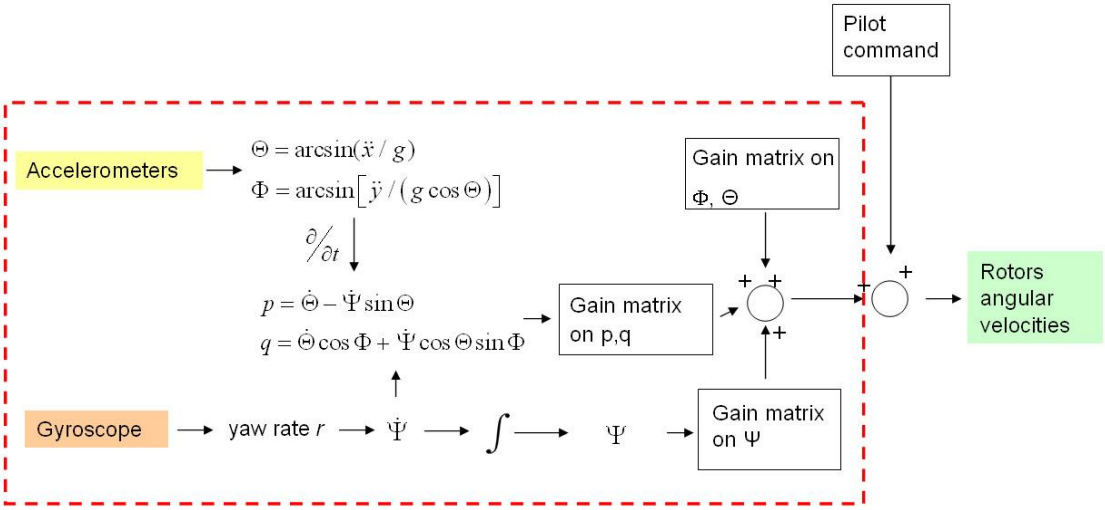

Figure 1. Controller board functional scheme as scheduled initially

Therefore, the control board has the ability to perform the aforementioned computation, the ability to manage different-channels signals inputted from the receiver, the accelerometers and the gyroscope and clearly the controller board perform the feedback.

As shown in Figure 1, the feedback acts on the attitude Euler angles and on the pitch and roll rates, to maintain the desired attitude; in the development phase the hover condition is chosen as a reference. The output feedback signals are added to the pilot command and the so-composed signals act increasing or decreasing the motor rpms.

In the first version of the controller board, currently installed on the quadrotor, the gyro does not work as expected thus it has been removed, neglecting the influence of the yaw rate and the yaw Euler angle. The error introduced is minimum, considering that the quadrotor is operating in hovering, thus the perturbation in attitude angles and angular velocities have to be limited. Usually, the contribution of the yaw angular rate is smaller than the pitch angular one.

The board feedback is a Proportional – Derivative (PD) controller; it has been decide to start with this controller due to its well known *modus operandi* The next step will be the implementation of a new control firmware; the L1 controller, described in the Section VI would be implemented, due to the possibility to vary the firmware.

The feedback gains can be modified through a specifically-developed software, which interface is shown in **Errore. L'origine riferimento non è stata trovata.**. The input IN_i are the signals from the transmitter, which range goes from -400 to +400, the output OUT_i are the angular velocities of each motors Ω_i. The yellow matrix correlate inputs and outputs whereas the cyan one embody the feedback gains. Moreover, the software allows to see in real-time the attitude angles, the angular rates and the acceleration along the three axes, from which angles and rates are derived.

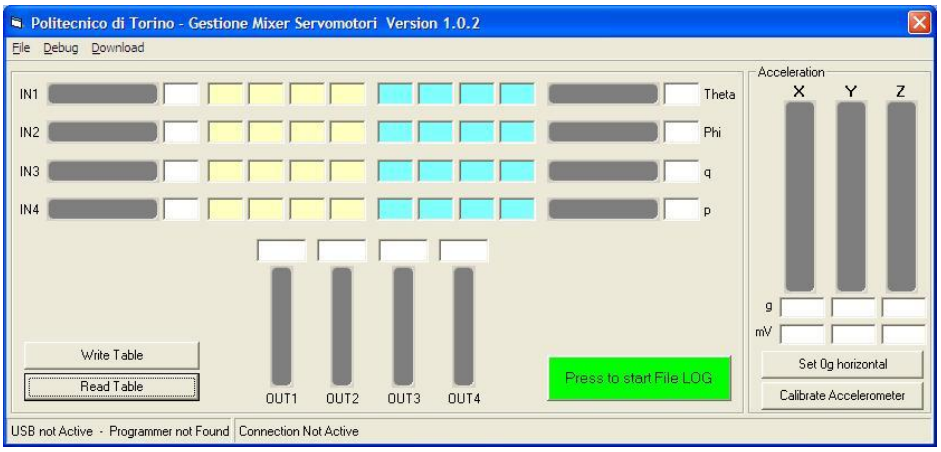

Figure 2. Motor management software interface

http://www.imavs.org/

http://www.imavs.org/

However, during the experimental activity, some noise is introduced in the signals, due to structural vibrations and to the numerical computation. For example, the trend of the angular rates contains some fluctuating disturbances and random glitches. To reduce this noise, a second-order finite difference formula has been implemented.

Therefore, a completely new controller board has been designed, again avoiding commercial products for the already aforementioned reason. The new layout is visible in Figure 3.

A three-axis gyroscope has been installed replacing the single-axes, thus all the angular rates are now measured directly, avoiding or at least reducing the noise originated by numerical derivation of attitude angles. Furthermore, a barometric sensor has been integrated to perform feedback on altitude, so having an altitude hold system. However, to date, the new controller board has not been embarked on the quadrotor due to trouble related to electromagnetic interference (EMI).

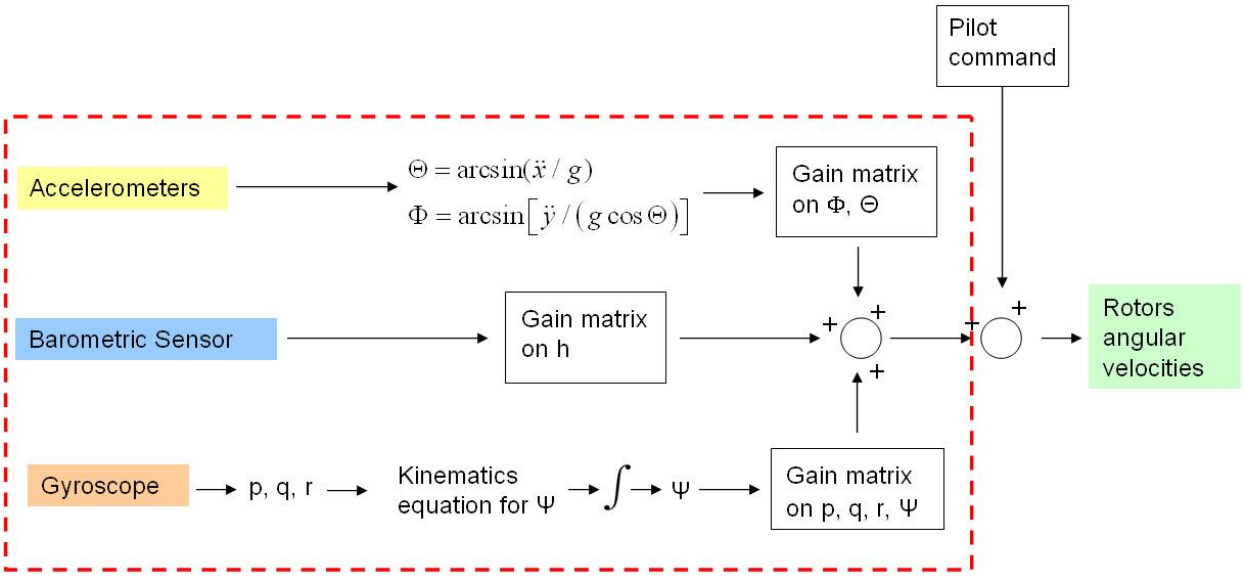

Figure 3. New-layout controller board functional scheme

III. The Mathematical Model

Taking into account the platform studied and its photogrammetric applications, a level 1 mathematical model is sufficient to define the simulation model. The level 1 defines the conventional six degree of freedom (DoF) flight mechanics formulation for the fuselage and the rotor dynamics are consolidated as a disc with coning and tilting freedoms. Unsteady (frequency dependent) aerodynamic effects are clearly ignored, due to the model implementation[6].

Table 1. Levels of rotor mathematical modelling

	Level 1	**Level 2**	**Level 3**
Aerodynamics	linear 2D dynamic inflow momentum theory	non linear (limited 3D) dynamic inflow momentum theory local effects of blade unsteady 2D compressibility	non linear 3D full wake analysis unsteady 2D compressibility
Dynamics	rigid blades quasi steady motion	rigid blades as in Level 1 limited number of blade elastic modes	detailed structural representation as elastic modes or finite element

To feedback the platform attitude, the operator has to interact in real time on the complete system. The data visualization is made with a Dynamic Data Exchange (DDE) transmission and a joystick block has to be defined on the Simulink model. The joystick sends step by step four commands (roll, pitch, yaw, throttle) with an absolute value of 1; the flight is controlled with a remote controller so a constant value has to be considered.

http://www.imavs.org/

Forces and moments have been computed in the most convenient reference frame, which subsequently were transformed in the body axes frame chosen to write the equations of motion. Many axes systems are needed inasmuch there is not a single axes system suitable for specifying all forces, moments, velocities, accelerations[7], therefore it was needed to define seven reference frames (in Figure 4 only five of them are visible for sake of clarity). To develop the mathematical model Ref. 8-11 were used.

Reference frame *F2* is centred in the hinge, if present, at the root at the blade, rotating with the blades, with X-axis from hub to tip, Y-axis 90 degrees advance with respect X-axis, Z-axis to form a right-hand system. Even the *F1* frame is hub centred and rotates with the blades, but its axes remain in the plane where the propeller is when does not turn, so it is called *partially-rotating* frame. Clearly, *F1* and *F2* frames differ between clockwise and counter-clockwise propellers.

The *non rotating* frame, not showed in Figure 4, is again hub prop centred but does not rotate; the *north-east-down* frame is in the CG of quadrotor centred as body axes frame; the latter has X-axis from CG towards rotors number 1, Y-axis towards number 4 and Z-axis to have a right-handed reference frame.

Some assumptions have been made: blades have been represented as infinitely rigid narrow bars, thus a point belonging to blade has been identified by a single coordinate, and aeroelastic phenomena have been neglected.

Differently from a rotor, the propellers do not have variable flapping nor lagging along the azimuth coordinate, because there is not the differential flow fields on advancing and retreating blades. Moreover, even when moving in forward flight the quadrotor pass through hover states, being the real phases of translational flights limited to short time; for the same reason the fuselage drag and the propeller velocity rate $\dot{\Omega}$ has been neglected. A quadrotor has neither cyclic and collective commands, nor flap and lag hinges. Therefore, the propeller blades present constant flap angle β and lag angle ζ. A final assumption provides blades work always far from stall conditions so a coefficient of lift-angle of attack linear-dependency exist.

After the definitions of the reference frames, the coordinate transformation matrices among the blade reference frame and from the body and partially rotating frames were computed. Clockwise and counter-clockwise rotors present different matrices, but here only those that deal with clockwise rotors have been reported.

The rotation angles between the blade frame, respectively between y-axes and x-axes, are the coning β and the lag ζ; those frames are useful to compute forces and moments acting on the blades. The coordinate transformation matrix is

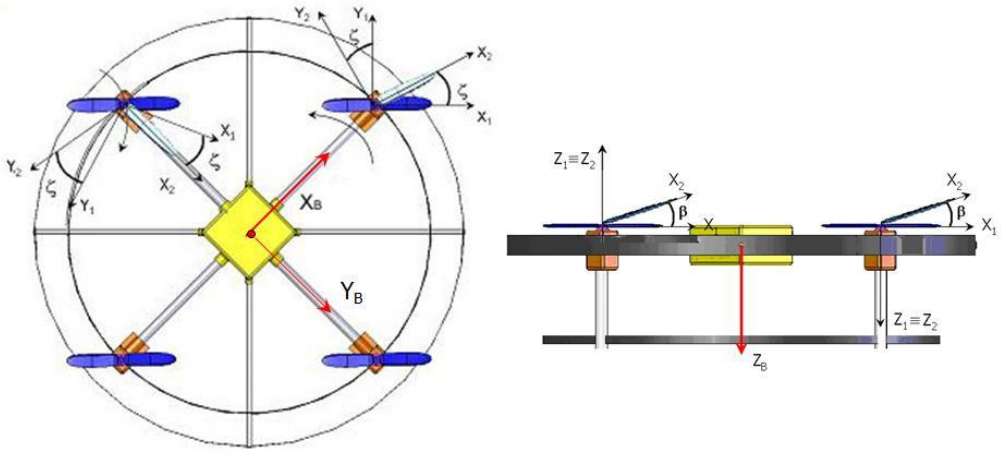

Figure 4. Reference frames for the development of mathematical model. The body-axes frame used to write the equations of motion are represented in red

$$[R]_{2c}^{1} = [R]_{\beta} \cdot [R]_{\zeta} = \begin{bmatrix} \cos\beta \cdot \cos\zeta & -\cos\beta \cdot \sin\zeta & -\sin\beta \\ \sin\zeta & \cos\zeta & 0 \\ \sin\beta \cdot \cos\zeta & -\sin\beta \cdot \sin\zeta & \cos\beta \end{bmatrix} \tag{2}$$

where subscript c identifies the matrix for clockwise turning propellers.
The matrix between body frame F_B and the partially-rotating frame F_1 is

$$[R]_{1c}^{B} = \begin{bmatrix} -\cos\psi & \sin\psi & 0 \\ \sin\psi & \cos\psi & 0 \\ 0 & 0 & -1 \end{bmatrix} \tag{3}$$

with $\Psi=\Omega t$ is the azimuth position of the blade.

Initially, the load acting on the blades, both aerodynamic and inertial ones, were computed using the classical method employed for helicopters[6], that is the loads were calculated at each revolution of the propellers integrating both along the blade radius and azimuth angles. Later this approach was dropped in the equations of motion due to its complexity and for a simulation in real time. Indeed, not having variable flap and lag along azimuth and in hover states, it is not necessary to compute the loads at each revolution of the propellers. However, the method has been used to compute the loads once a time to evaluate their magnitude for different rpm of the propellers, thus it has been resumed in the following paragraphs.

A. Inertial forces and moments acting on the blades

Infinitesimal inertial forces F^i and moments M^i, acting on a point belonging to the blade, have been computed using

$$d\vec{F}^{\,i} = -dm \cdot \vec{a}_p \tag{4}$$

$$d\vec{M}^{\,i} = \vec{r}_0 \times d\vec{F}^{\,i} = -\vec{r}_0 \times \vec{a}_p \cdot dm \tag{5}$$

where dm is an infinitesimal mass, a_p is the acceleration and r_0 is the moment arm. Due to constant flap and lag angles and the practically absence of forward flight the inertial loads have been resulted negligible.

B. Aerodynamic forces and moments acting on the blades

Lift and drag have been calculated on an infinitesimal strip of blade using

$$dL = \frac{1}{2} \cdot \rho \cdot c \cdot R \cdot U_0^2 \cdot C_L \cdot dx \tag{6}$$

$$dD = \frac{1}{2} \cdot \rho \cdot c \cdot R \cdot U_0^2 \cdot C_D \cdot dx \tag{7}$$

where ρ is the air density, c is the blade mean aerodynamic chord, R is the radius, U_0 is the asymptotic air speed, C_L and C_D respectively the lift and drag coefficients of the blade airfoil and dx is the wide of a non-dimensional blade infinitesimal strip. With the assumptions done C_L is linear-related to angle of attack and C_D is computable with the quadratic polar.

Only the scheme of forces and moments for a clockwise propellers is depicted in Figure 5, taking into account that for counter-clockwise propellers the process is equal but with different coordinate transformation matrices. It has been more convenient to compute the velocity U_0 in reference frame *F1* so the sequence of calculation has been:

- the speed was computed in frame F1
- this speed was substituted in Eqs. (6) and (7)

http://www.imavs.org/

- the infinitesimal lift and drag were decomposed along reference frame *F2* and were integrated along the blade.

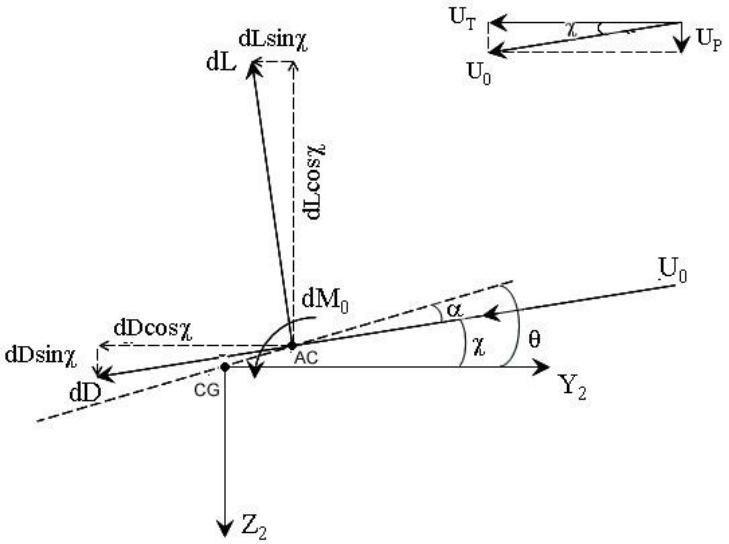

Figure 5. Forces and moments on the clockwise rotating blades

Thus the final relationships, as example for aerodynamic forces along Y_2-axis, became in the form of

$$F_{y2}^{A} = -\frac{1}{2} \cdot \rho \cdot c \cdot R \cdot \left(\int_0^1 U_0^2 \cdot C_L \cdot \sin\chi \cdot dx + \int_0^1 U_0^2 \cdot C_D \cdot \cos\chi \cdot dx \right) \tag{8}$$

with χ indicating the climb angle.

Asymptotic speed U_0 was obtained by the composition of three velocities: the blade speed, due to its rotating motion; the quadrotor speed, which is zero in hovering, and the propeller induced inflow. It is noteworthy that the Eq. (8) contains both time- and space-dependent terms correlated each other, being linked by the blade azimuth position Ψ.

An analytical solution was investigated to calculate the aerodynamic forces and moments, as reported in Eq. (8), i.e. in the most rigorous mode. To simplify the computational time, the aerodynamic loads were calculated expressing the to-be-integrated equations, as Taylor-series-expansion around zero (small angles of attack considered), for different propeller rpm. Instead, the integral solutions result in stepwise-equations, which were not useful to implement in the equations of motion.

However, this approach has been useful to evaluate, without demanding resources, the magnitude of the aerodynamic forces and moments along F2-frame. The only aerodynamic loads not negligible are acting on Z-axis, that is the thrust and the reaction torque.

Another method[12] has been used to estimate the aerodynamic loads on the propeller, to verify that the only loads noteworthy is along Z-axis. Subsequently, torque and force varying with rpm were measured experimentally.

http://www.imavs.org/

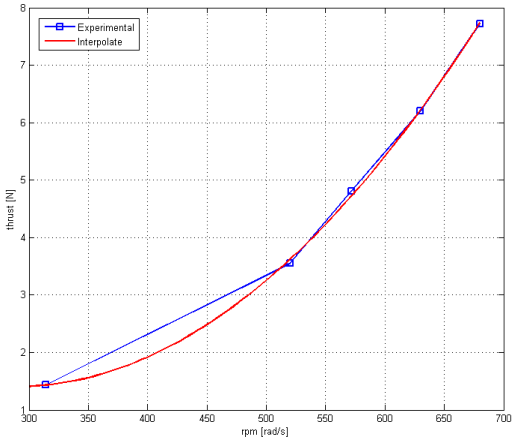

Figure 6. Thrust vs rpm

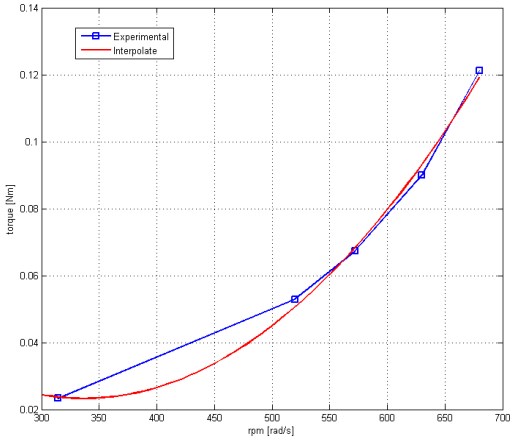

Figure 7. Torque vs rpm

Both the method employed have been useful to demonstrate the other loads acting on the blades were negligible because the available experimental setup did not permit to measure them. The graphs in Figure 6 and Figure 7 show torque and thrust plotted against Ω measured experimentally and subsequently used in the mathematical model. In the lower rpm zone a gap exists from experimental and theoretically values, the latter represented with a curve obtained interpolating the experimental data; the gap is due to less data points obtained at such low propellers speed.

C. Equations of motion

The equation of motion written with respect to body reference frame are reported in Eqs. (9-14). The equations are written already considering that the inertial tensor is diagonal due to the quadrotor symmetry and that drag of structure, when the quadrotor is in forward flight, has been neglected, as aforementioned above; thus the only loads acting are the thrust, the reaction torque and the weight.

To complete the mathematical model the kinematic equations to describe the Euler angles rate[7,10] have to be added, but they have not been reported here. As usually in flight dynamics[7,10], the Earth rotation about its own axis and its curvature have been neglected.

$$\dot{u} = vr - wq + g\sin\Theta \tag{9}$$

$$\dot{v} = wp - ur + g\sin\Phi\cos\Theta \tag{10}$$

$$\dot{w} = uq - vp + g\cos\Phi\cos\Theta - \frac{T_1 + T_2 + T_3 + T_4}{m} \tag{11}$$

$$\dot{p} = \frac{1}{I_x}\left[\left(T_2 - T_4\right)\frac{d}{2} - qr\left(I_z - I_y\right)\right] \tag{12}$$

$$\dot{q} = \frac{1}{I_y}\left[\left(T_1 - T_3\right)\frac{d}{2} - pr\left(I_x - I_z\right)\right] \tag{13}$$

$$\dot{r} = \frac{1}{I_z}\left[C_1 - C_2 + C_3 - C_4 - pq(I_y - I_x)\right] \tag{14}$$

http://www.imavs.org/

where u, v, w are the linear velocities, m is the quadrotor mass, T_i are the i-th motor thrusts, C_i are the i-th motor reaction torques, I_x I_y I_z are the moment of inertia with respect to the body axes, d is the distance from each motors and the quadrotor center of gravity.

IV. Simulation results and experimental flight tests

Some numerical simulations are made to validate the mathematical model. The hovering is considered as a reference maneuver; thus the Euler angles and the angular velocities has to be null.

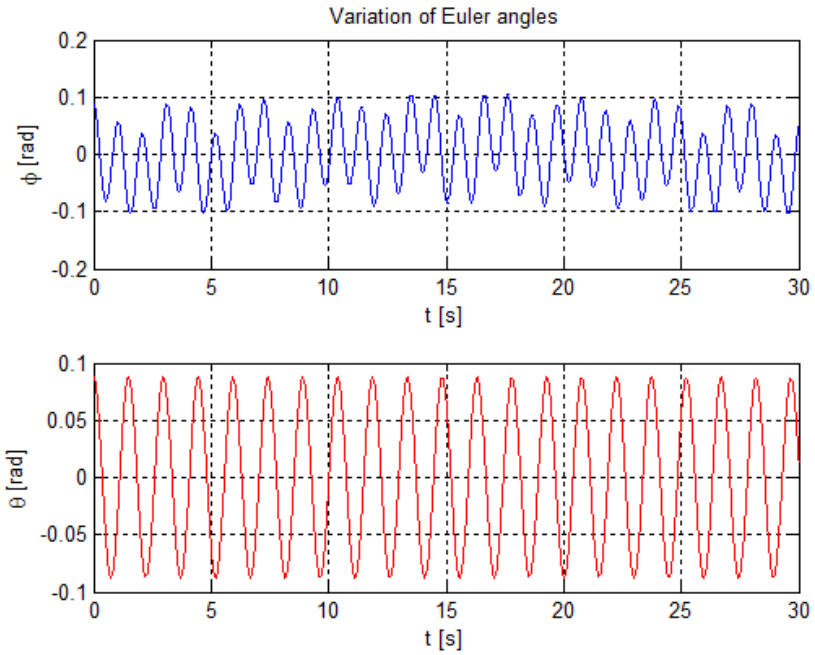

Figure 8. Trend of the Euler angles without a feedback

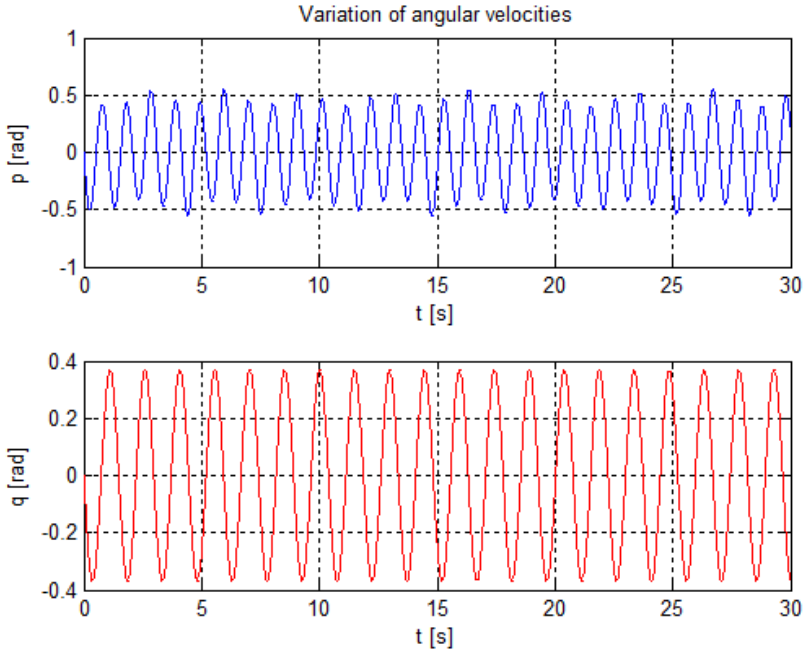

Figure 9. Trend of the roll and pitch rates with no feedback

http://www.imavs.org/

The graphs above represents the platform response, when no feedback is applied. As mentioned before, the quadrotor is unstable, if a maneuver is imposed without a controller. The platform must be stable after a given disturbance, moving back attitude initial conditions.

To damp the oscillation and to reduce the steady state error, a PD controller is necessary, as implemented on the controller board.

The final gain scheduling is in Table 2.

Table 2. Gain scheduling

Proportional controller	
ϕ gain	-1.6
θ gain	-0.6
PD controller	
ϕ gain	-0.8
θ gain	-1.2
p gain	-0.2
q gain	-0.8

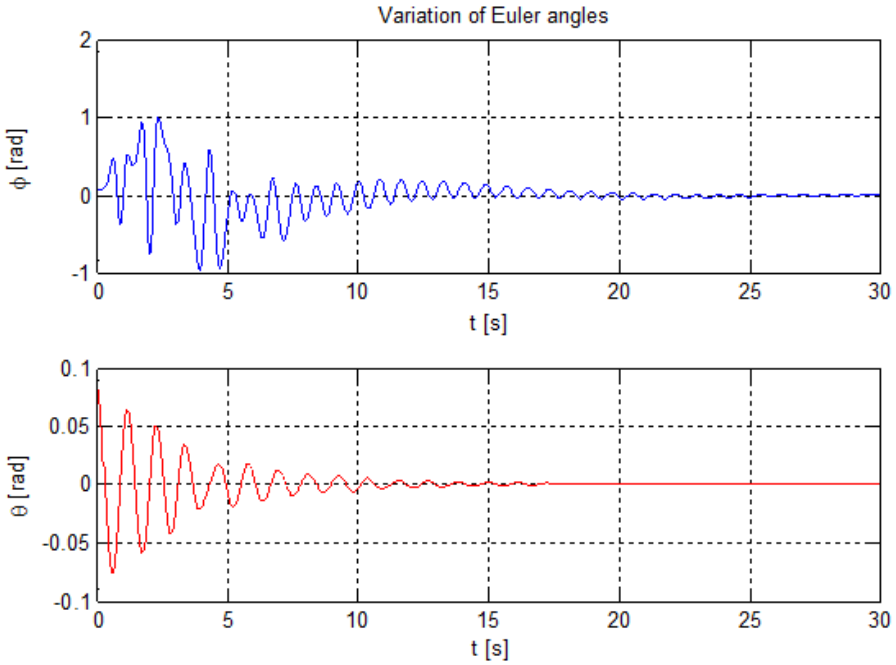

Figure 10. Variation of the Euler angles with a PD controller

http://www.imavs.org/

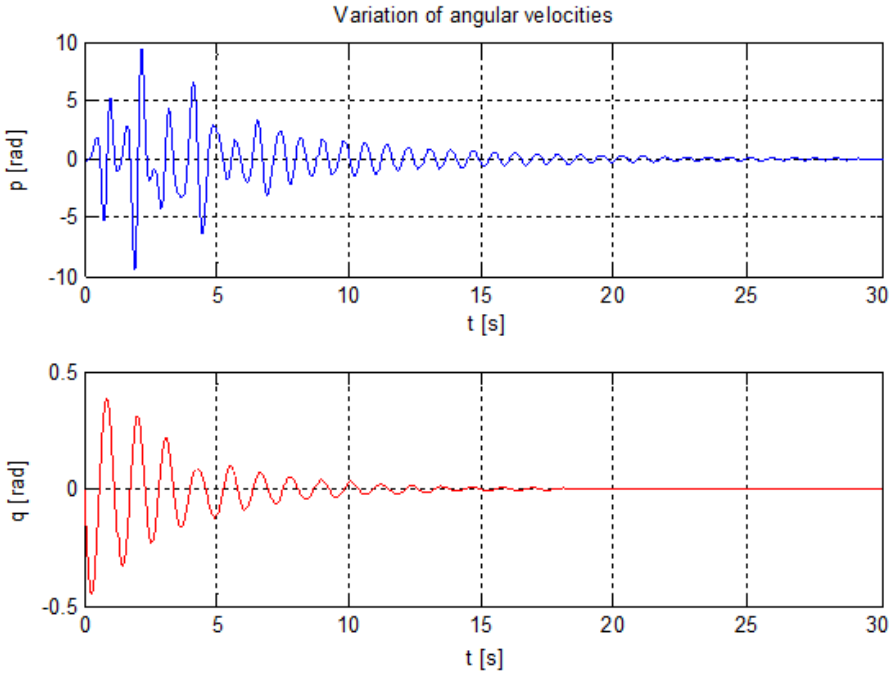

Figure 11. Angular velocities variation with a PD controller

As indicated above, the feedback on the yaw angle and rate is not considered, because no feedback on these parameters is implemented. In the graphs above, after a oscillation trend in the first seconds of simulation, the platform can perform a hovering manoeuvre, with null angular velocities and Euler angles.

If the same gain scheduling is imposed on the controller board and a hover manoeuvre is considered, the following results are obtained. As indicated in Session II, due to the structural vibrations and derivation noise, the two responses are not totally comparable. If the attention is focused on the general trend of the variables, the responses are similar, but they are not optimized.

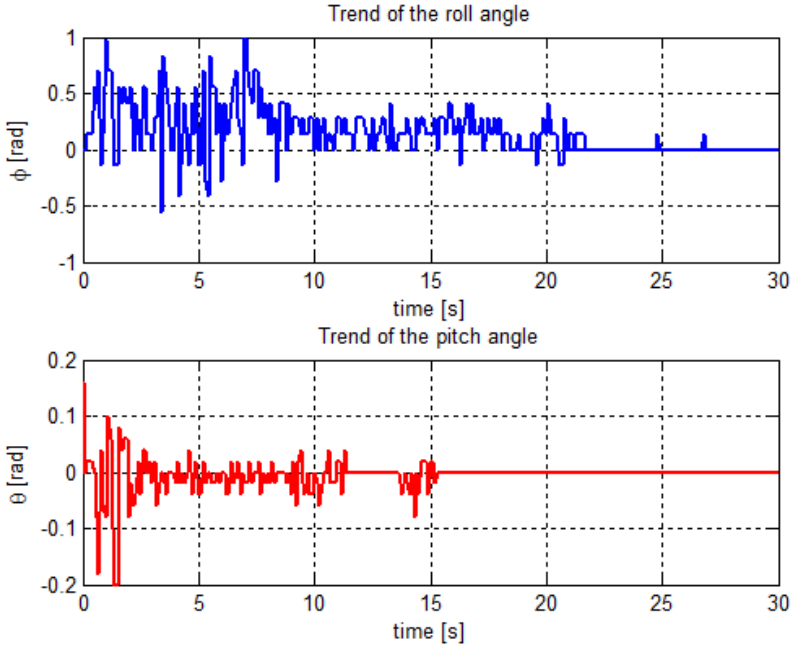

Figure 12. Experimental trend of the roll and pitch angles

http://www.imavs.org/

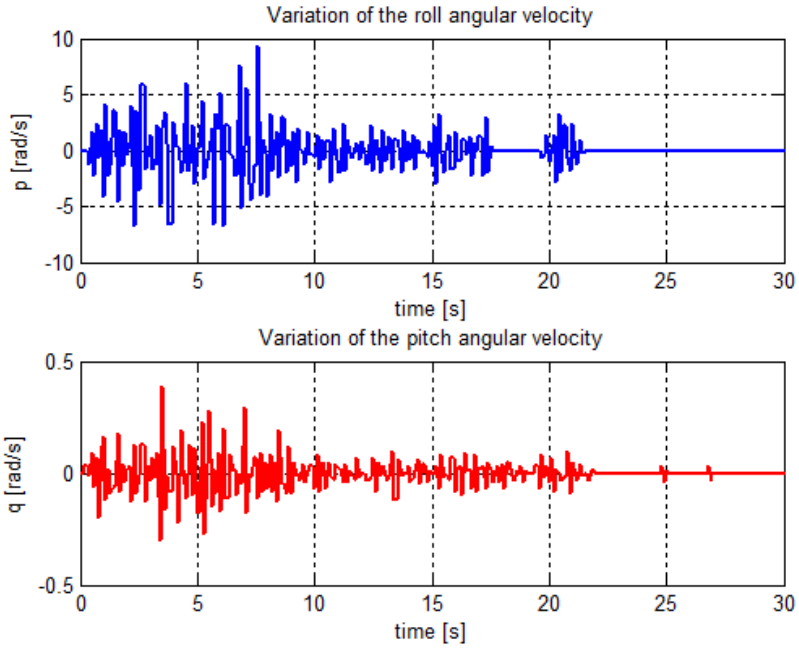

Figure 13. Experimental trend of the roll and pitch angular velocities

The platform Euler angles have a rise time of about 10 seconds, that is not adequate for a platform of this dimensional and dynamic characteristics. In the roll angular rate, if a filter is not applied, a maximum overshoot of about 10 rad/s is reached; this is due to the aforementioned numerical evaluation (a second-order finite difference formula). A low pass-filter has to be implemented on the controller board, to avoid numerical noise.

At this level the results obtained are not enough exhaustive, due to the slow response when a perturbation has occurred on the platform.

V. Dynamic Analysis and Eigenstructure assignment

In order to implement an optimal controller, the purpose is to express the equations of motion in the state-space form, deriving linear, constant-coefficient state and output equations. The quadrotor dynamic stability, as a first approximation, is analyzed in hovering conditions. For the complete description of the equations and stability analysis see [13].

The stability derivatives are usually presented as the ratio of the force changes divided by the aircraft mass and the moment changes about each axis divided by the appropriate moment of inertia[8].

An important derivative, that has to be considered in order to evaluate the longitudinal stability analysis, is M_w. This is called static stability derivative and it represents the change in pitching moment about the aircraft centre of mass, when the platform is subject to a perturbation in normal velocity w or in incidence.

If M_w is positive, the aircraft is defined statically unstable in pitch; if M_w is negative then the aircraft is statically stable[6]. For a quad-rotor, this parameter is very configuration–dependent and it is also a function of perturbation amplitude. The coupled pitch-heave motion is a critical approximation for a multi rotor UAV and has a limited range of applications due to the strong coupling with speed variations, reflected in the speed derivatives M_u. This speed derivative is significant even in hovering condition and it can contributes to the dynamic instability of the phugoid mode[14]. In this case, $M_w = 0$ so the pitch and heave motions are uncoupled given two first order transients (the decay rate is given by the derivatives Z_w and M_q).

A simple case for which the motion can be assumed decoupled is the motion around the yaw axis when in hover. The time history of the spiral mode is an oscillatory convergence[15]. The sign of the constant term in the characteristic equation of lateral directional plane determines the mode stability.

For a complete controller, the study of the two separate plane results incomplete; for this reason the cross-coupling derivatives are calculated and the assumption of decoupled planes has to be dropped.

A desirable property of a system design is that the poles should be insensitive to perturbations in the coefficient matrices of the system equations; this criterion is considered to produce a well-conditioned or robust solution. The

http://www.imavs.org/

feedback matrix is obtained by assigning linearly independent eigenvectors as well-conditioned as possible. The system behaviour in state space formulation is governed by the platform poles[16].

The pole placement has been made considering the desired dynamic specifications.

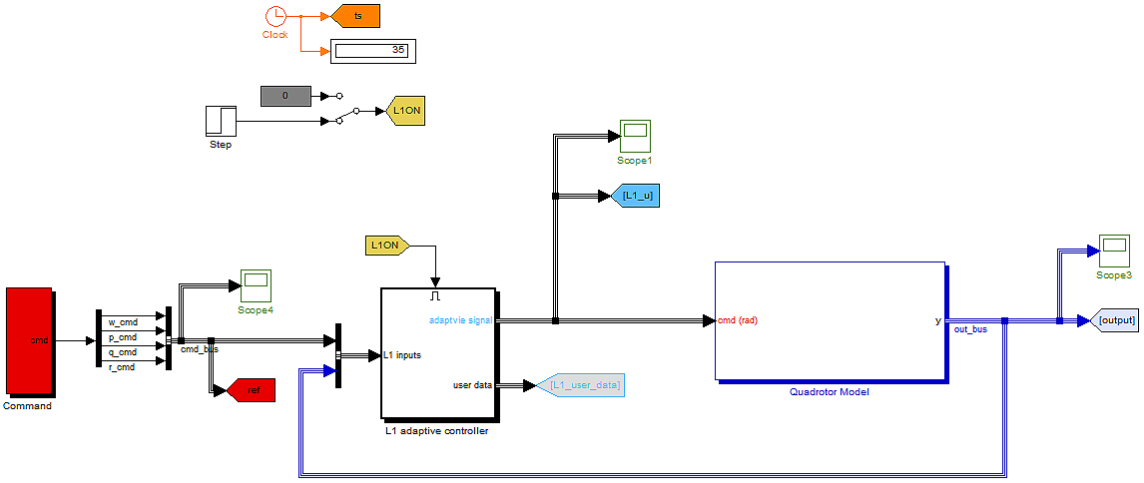

Figure 14. Simulink model including the L1 adaptive controller

VI. L1 adaptive controller

There are many reasons why researchers prefer adaptive laws to find control signals, especially for non-linear problems for which an analytical solution is barely possible. Uncertainties in the system, disturbances, and measurement noise are some of these reasons. The L1 adaptive strategy has recently been introduced by Cao and Hovakimyan[17,18]. This new approach presents better results, especially during the transient phase. It can provide robust performance against external disturbances and measurement noises. Some advantages of the L1 adaptive architecture are the improved asymptotic tracking and the guaranteed time-delay margin, achieved via smooth control input.

The L1 adaptive control approach replaces the conventional model reference adaptive control (MRAC) by first specifying an equivalent model architecture, which enables an insertion of a low-pass filter in the closed loop. Without a low-pass filter the reference signal, including the high frequencies component, is passed exactly to the control channel. The filter is introduced with the understanding that uncertainties in any feedback loop can only be compensated for within the bandwidth of the control channel. The decoupling between fast adaptation and robustness, inherent to all L1 adaptive control architectures, is achieved via the introduction of this low-pass filter on the adaptive control signal.

L1 adaptive control theory's systematic design procedures also significantly reduce the tuning effort required to achieve desired closed-loop performance, particularly while operating in the presence of uncertainties and failures.

The elements of the L1 adaptive controller are the state predictor, the adaptive law and the control law. The state predictor is defined similar to the plant equations, but replacing the unknown variables by their estimates. This adaptive controller is based on a piecewise constant adaptive law and defines a state predictor to estimate the uncertainties[19].

The problem formulation is:

$$\begin{cases} \dot{x}(t) = A_m x(t) + B_m K_g u(t), \quad x(0) = x_0 \\ y(t) = Cx(t) \end{cases} \tag{15}$$

x(t) is the system state vector (measured), u(t) is the control signal, y(t) is the regulated output and A_m is a known Hurtwiz matrix that defines the desired dynamics for the closed-loop system, B_m and C are known constant matrices.

Assumption 1: There exists a control matrix K_n such that $A_m = A - BK_n$ is Hurwitz. The matrix K_n is calculated from the pole placement theory[16]

http://www.imavs.org/

The control objective is to design an adaptive state feedback controller in order to guarantee that the output y(t) tracks the response of a desired system $M(s) \hat{=} C(sI - A_m)^{-1} B_m K_g(s)$, where $K_g(s)$ is a feedforward pre-filter. This filter is a constant matrix where the diagonal elements of the desired transfer matrix *M(s)* have DC gain equal to 1, while the off-diagonal elements have zero DC gain.

The prefilter $K_g(s)$ can be calculated starting from the matrix A_m and B_m, as follows

$$K_g(s) \equiv K_g = -\left(CA_m^{-1}B_m\right)^{-1} \tag{16}$$

The state predictor can be written as

$$\dot{\hat{x}}(t) = A_m \hat{x}(t) + B_m\left(u(t) + \hat{\sigma}_m(t)\right) \tag{17}$$

where B_m = B because only the hover maneuver has been consideres and $\hat{\sigma}_m(t)$ is the vector of matched eigenvalues.

For a model design, the effects of slow outer-loop variables may appear as unmatched uncertainties in the dynamics of the fast inner-loop variables that are regulated.

The adaptation law for $\hat{\sigma}_m(t)$ is defined as

$$\hat{\sigma}_m(t) = -B^{-1}\Phi(T_s)\exp^{A_m T_s} \tag{18}$$

where T_s is the sampling time and $\Phi(T_s)$ is a square matrix given by

$$\Phi(T_s) = A_m^{-1}\left(\exp^{A_m T_s} - I_n\right) \tag{19}$$

As a final step, the control law has been considered. The control signal is the output of the following system

$$\begin{cases} u(t) = -K_n D(s)\hat{\eta}(s) \\ \hat{\eta}(s) = u(t) + \hat{\sigma}_m(t) - K_g(s) r(s) \end{cases} \tag{20}$$

where $D(s)$ is an identity matrix and r is a reference signal.

http://www.imavs.org/

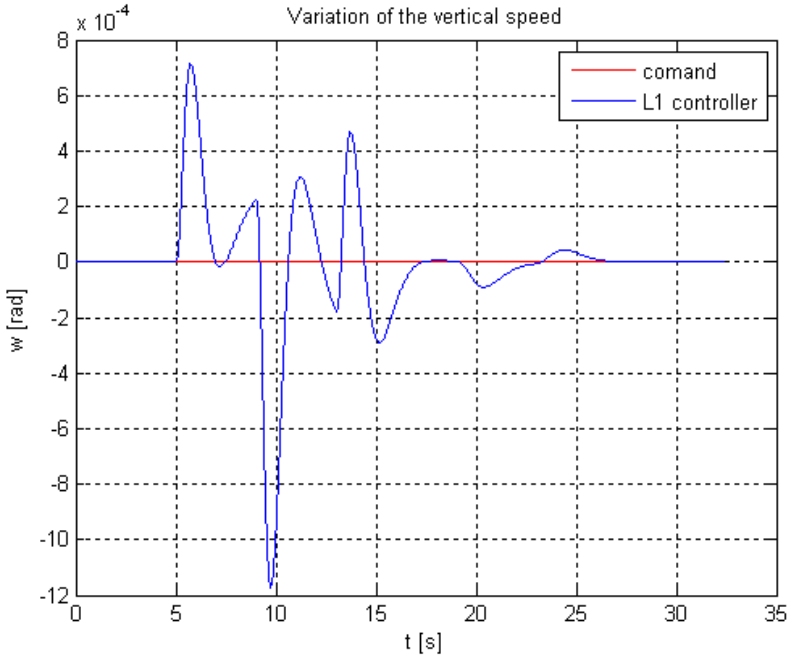

Figure 15. Variation of the vertical speed

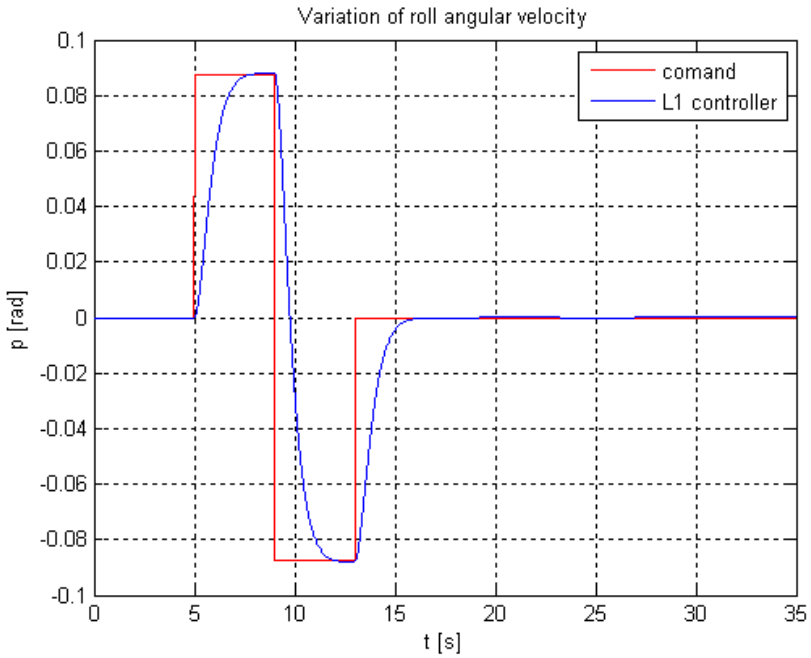

Figure 16. Trend analysis of roll angular rate

http://www.imavs.org/

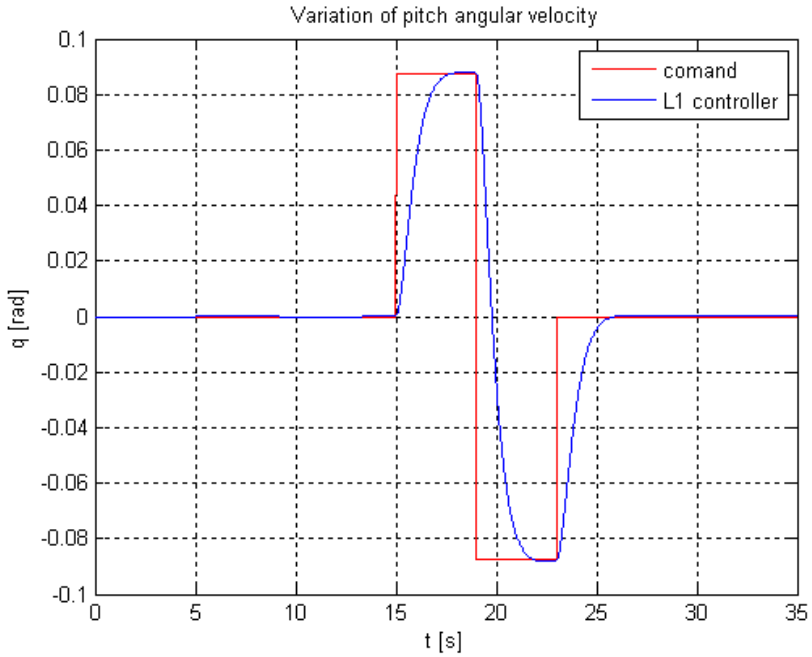

Figure 17. Pitch angular rate trend

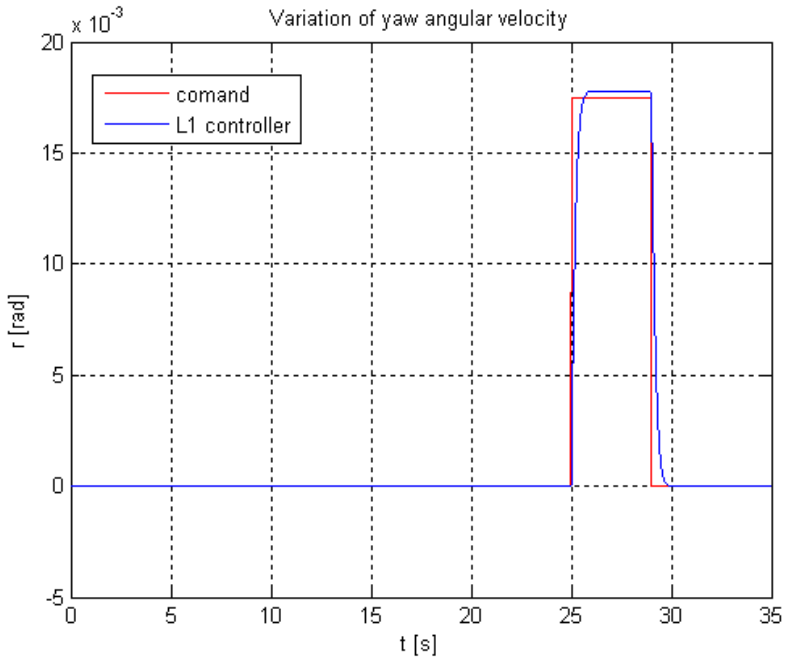

Figure 18. Variation of the yaw angular rate

Setting as a reference a doublet maneuver for the p and q variations, a step for the yaw angular velocity and a null variation for the vertical speed (corresponding to the hovering), the simulation results have been reported in the figures above.

With the L1 controller the platform can perform a fast maneuver in the three axis, even if there are small oscillations on the vertical speed. The controller is implemented in hover but, using a gain scheduling on the speed variation, the model can be implemented in different flight conditions, without the tuning of the model matrices. The

http://www.imavs.org/

responses can be improved with a different pole placement, but the actuators characteristics and the system performances have to be considered.

VII. Conclusion

At Politecnico di Torino Aerospace Engineering Department a quadrotor is under development for territorial monitoring applications and as flying test bed for different feedback control systems.

Some experiments have been carried out with a PD controller to validate the developed mathematical model and they demonstrated that, except for noise due to structural vibration, the simulations performed in Matlab/Simulink matched partially with the real behavior of the quadrotor. The response is dynamically stable and, after a perturbation, the aircraft is moving back the trim conditions.

To optimize the experimental results and to eliminate the derivation noise, some simulations with a L1 controller have been carried out but it has not been yet possible to verify experimentally if the controller works as expected.

The philosophy of a L1 controller is to introduce separation between adaption and robustness. This controller defines the control signal as the output of a low pass-filter to guarantee that the control signal stays in the low-frequency range. The controller state matrix is based on the pole placement theory and it is possible to demonstrate that the adaptive controller is applicable in different flight operations with the same gain matrix.

The next step includes the validation of the stability characteristics in remote control. With the controller board it can be demonstrated that the gain matrix K_n and the adaptive algorithm are compatible and if the simulation results are similar to the experimental ones. A new controller board will be designed, implementing a L1 customized control algorithm.

http://www.imavs.org/

Acknowledgments

The authors thank the Prof. Naira Hovakimyan and her group at the University of Urbana – Champaign (Illinois, USA) for sharing experience and knowledge on the L1 controller theory and implementation.

References

[1]Guernard, N., Hamel, T., Moreau, V. Dynamic Modelling and Intuitive control strategy for an X4 flyer. *International Conference on Control and Automation*, Budapest, Hungary, 2005

[2]Mc Kerrow, P. (2004). Modelling the Draganflyer four-rotor helicopter. *IEEE International Conference on Robotics and Automation.* New Orleans (USA).

[3]Castillo, P., Dzul, A., and Lozano, R., "Real-Time Stabilization and Tracking of a Four-Rotor Mini Rotorcraft", *IEEE Transactions On Control Systems Technology*, Vol. 12, No. 4, July 2004

[4]Pounds, P., Mahony, R, Hynes, P, and Roberts, J, "Design of a four-rotor aerial robot", *Australasian Conference on Robotics and Automation*, Auckland, 27-29 Novembre 2002

[5]Capello, E., Guglieri, G., & Quagliotti, F. (2009). A design configuration and optimization for a multi rotor UAV. *NATO RTO Symposium Intellignet Uninhabited Vehicle Guidance Systems.* Neubiberg/Munich (Germany).

[6]Padfield, G. D., *Helicopter Flight dynamics: The theory and Application of Flying Qualities and Simulation Modelling*, Blackwell Publishing, March 2007

[7]Pamadi, B. N., *Performance, Stability, Dynamics, and Control of Airplanes*, 2nd ed., AIAA Education Series, 2004

[8]Prouty, R. W., *Helicopter Performance, Stability, and Control*, Krieger Publishing Company, Malabar, Florida, 2005

[9]Stevens, B. L., and Lewis, F. L., *Aircraft Control and Simulation*, John Wiley and Sons Inc., 2003

[10]Etkin, B, and Reid, L. D., *Dynamics of Flight: Stability and Control*, 3rd ed, John Wiley & Sons, Nov 1995

[11]Johnson, W., *Helicopter Theory*, Dover Books, 1994

[12]Flachsbart, O., and Krober, G., "Experimental investigation of aircraft propellers exposed to oblique air currents", NASA Technical Report, 1929

[13]Capello, E., Guglieri, G., & Quagliotti, F. (under review). Hovering dynamic stability and adaptive control for a small quad-rotor UAV. *Aerospace Science and Technology*.

[14]Padfield, G. (1981). On the use of approximate models in Helicopter Flight Mechanics. *VERTICA* , vol. 5 pp. 243-259.

[15]Sinclair, S., & Kereliuk, S. (1983). Evaluation of the Effects of Lateral and Longitudinal Aperiodic modes on Helicopter Instrument Flight Handling Qualities. *NAEAN-15, Canada* .

[16]Kautsky, J., Nichols, N. K., & Van Dooren, P. (1985). Robust pole assignment in linear state feedback. *International Journal of Control* , vol.41, pp. 1129-1155.

[17]Cao, C., & Hovakimyan, N. (2006). Design and analysis of a novel L1 adaptive controller, Part 2: Guaranteedtransient performance. *Proceedings of the 2006 American control conference*, (p. 3403-3408). Minneapolis, Minnesota.

[18]Cao, C., & Hovakimyan, N. (2006). Design and analysisof a novel L1 adaptive control architecture, Part 1:Control signal and asymptotic stability. *Proceedings of the 2006 American control conference*, (p. 3397-3402). Minneapolis, Minnesota.

[19]Xargay, E., Hovakimyan, N., & Chengyu, C. (2010). Piecewise Constant Adaptive Laws for L1 Adaptive Controller in the Presence of Uncertain Nonlinear Cross- Coupling. *American Control Conference*, (p. submitted). Baltimore (USA).